Electronic Structure and Unusual Exchange Splitting in the Spin-Density-Wave State of the $BaFe_2As_2$ Parent Compound of Iron-Based Superconductors

L. X. Yang,[1] Y. Zhang,[1] H. W. Ou,[1] J. F. Zhao,[1] D. W. Shen,[1] B. Zhou,[1] J. Wei,[1] F. Chen,[1] M. Xu,[1] C. He,[1] Y. Chen,[1] Z. D. Wang,[1,2] X. F. Wang,[3] T. Wu,[3] G. Wu,[3] X. H. Chen,[3] M. Arita,[4] K. Shimada,[4] M. Taniguchi,[4] Z. Y. Lu,[5] T. Xiang,[6] and D. L. Feng[1,*]

[1]*Surface Physics Laboratory (National key laboratory), Physics Department, and Advanced Materials Laboratory, Fudan University, Shanghai 200433, People's Republic of China*
[2]*Department of Physics, The University of Hong Kong, Hong Kong, People's Republic of China*
[3]*Hefei National Laboratory for Physical Sciences at Microscale and Department of Physics, University of Science and Technology of China, Hefei, Anhui 230026, People's Republic of China*
[4]*Hiroshima Synchrotron Radiation Center and Graduate School of Science, Hiroshima University, Hiroshima 739-8526, Japan*
[5]*Department of Physics, Renmin University of China, Beijing 100872, People's Republic of China*
[6]*Institute of Physics, Chinese Academy of Sciences, Beijing 100190, People's Republic of China*

(Received 6 July 2008; published 11 March 2009)

The magnetic properties in the parent compounds are often intimately related to the microscopic mechanism of superconductivity. Here we report the first direct measurements on the electronic structure of a parent compound of the newly discovered iron-based superconductor, $BaFe_2As_2$, which provides a foundation for further studies. We show that the energy of the spin density wave in $BaFe_2As_2$ is mainly lowered through exotic exchange splitting of the band structure.

DOI: 10.1103/PhysRevLett.102.107002 PACS numbers: 74.25.Jb, 71.20.−b, 74.70.−b, 79.60.−i

The discovery of superconductivity in iron-pnictide has generated another intensive wave of research on high temperature superconductivity [1–5]. The record superconducting transition temperature (T_c) has been quickly raised to 56 K in $LnO_{1-x}F_yFeAs$ (Ln = La, Sm, Nd, etc.), and a T_c of 38 K has been reported in $Ba_{1-x}K_xFe_2As_2$ [6,7]. Intriguingly, like in the cuprates, the ground state of the parent compound LaOFeAs is a magnetically ordered spin-density-wave (SDW) state [8]. Similarly, $BaFe_2As_2$ enters the SDW phase at the transition temperature T_S of around 138 K [9,10]. Currently, it is unclear whether the SDW facilitates the electron pairing as the antiferromagnetic fluctuations arguably do in cuprates, or acts as a competing order as the charge density wave does in transition metal dichalcogenides. Therefore, it is crucial to reveal the nature of the SDW and its manifestation on the electronic structure.

We here report angle resolved photoemission spectroscopy (ARPES) data of $BaFe_2As_2$ single crystals. In the paramagnetic state, we found that the Fermi surfaces (FS's) are consisted of two hole pockets around the Brillouin zone center Γ of the tetragonal unit cell, and one electron pocket at the zone corner M. This qualitatively resembles the density functional theory (DFT) electronic structure calculations on LnOFeAs [11–15] and $BaFe_2As_2$ [16]. In addition, we observed renormalization of the band structure due to the correlation effects. Below T_S, band splitting and folding are observed, which induces several additional FS's. We show that the exchange splitting of the band structure lowers the total electronic energy effectively, and could induce the SDW. In addition, signs of possible gap opening are observed at certain bands, which suggests FS nesting might also play a role in the SDW formation.

The $BaFe_2As_2$ single crystals were synthesized and characterized as described in Ref. [9] with $T_S = 138$ K. ARPES measurements were performed with photons from beam line 9 of Hiroshima synchrotron radiation center, and 21.2 eV photons from a helium-discharge lamp. Scienta R4000 electron analyzers are equipped in both setups. The overall energy resolution is 10 meV, and angular resolution is 0.3°. The samples were cleaved in ultrahigh vacuum, and the surface quality is confirmed by low energy electron diffraction.

Photoemission intensity at the Fermi energy (E_F) is a direct measure of the FS's. Figure 1(a) shows the normal state map of the photoemission intensity: there are features around both the Γ and M points. Figures 1(b), 1(b1), and 1(b2), illustrate the photoemission intensity, energy distribution curves (EDC's) and momentum distribution curves (MDC's) across the momentum cut no. 1 in Fig. 1(a) through Γ. Two bands (assigned as Γ_A and Γ_B band, respectively) could be identified to cross E_F, giving two hole-type FS's around Γ. In addition, there is a feature near 200 meV below E_F. On the other hand, Figs. 1(c) and 1(c1) illustrate the photoemission intensity and EDC's along the cut no. 2 in Fig. 1(a) through M. The spectra are dominated by a strong feature dispersing toward M. However, a weak feature near E_F could be resolved in the normalized MDC's (indicated by bars in Fig. 1(c2), see caption for description). By tracking these features in MDC's and EDC's, we identified two bands in Fig. 1(c) (see dashed lines for guide): the band at higher binding

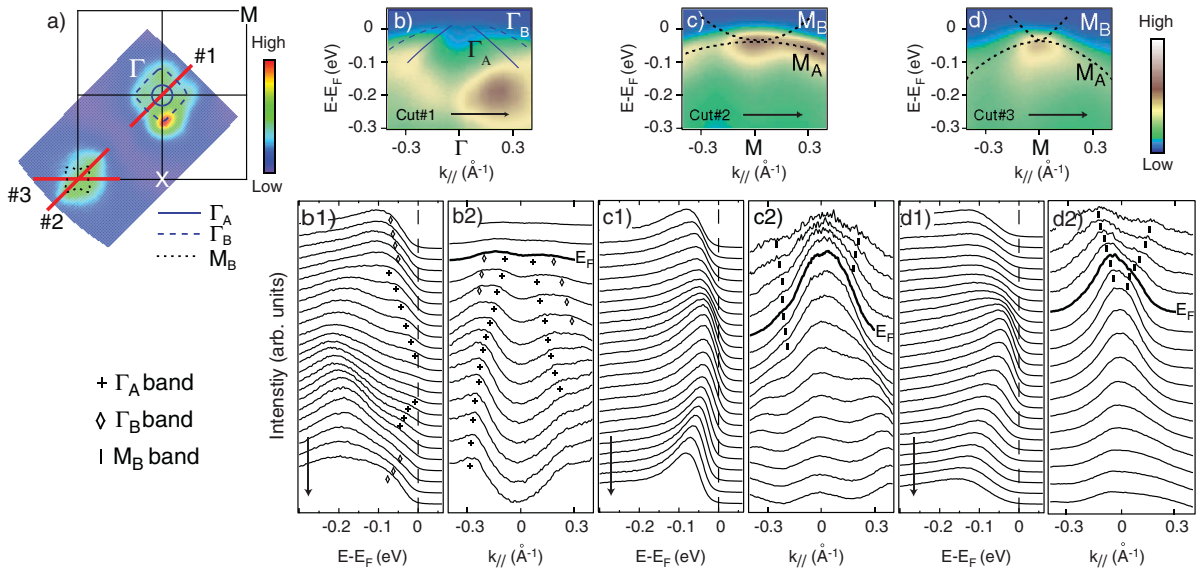

FIG. 1 (color). Normal state FS and band dispersion of $BaFe_2As_2$. (a) Photoemission intensity map in the Brillouin zone at E_F. The dashed lines are the measured FS's. (b) Photoemission intensity along cut no. 1 through Γ as indicated in panel a, and the corresponding (b1) EDC's, and (b2) MDC's. (c) Photoemission intensity along cut no. 2 through the zone corner M, and the corresponding (c1) EDC's, and (c2) MDC's after individually normalized by its integrated weight. (d) Photoemission intensity along cut no. 3 through the zone corner M, and the corresponding (d1) EDC's, and (d2) normalized MDC's. The energy difference between two neighboring MDC's is 9 meV. Data were taken at 160 K with 21.2 eV photons at the synchrotron.

energies is below E_F (named as M_A band), while the other one crosses E_F (named as M_B band), which corresponds to the electronlike pocket around M in Fig. 1(a). Figures 1(d), 1(d1), and 1(d2) illustrate similar behavior along the MX direction (cut no. 3), except that the Fermi crossings are closer.

The measured bands qualitatively agree with the DFT calculations [11–17], however, there are quantitative discrepancies. For example, the bottom of the normal state M_B are about 20–30 meV below E_F, while the top of the Γ bands is estimated to be at most 50 meV above E_F, if the measured dispersion is extrapolated to Γ. Thus their separation is about 70–80 meV, while it is approximately 300–400 meV in various band calculations, indicating certain correlation effects that likely missing in the calculations.

The SDW effects are examined by the temperature dependence of the bands, which could be tracked in the second derivative of the photoemission intensity with respect to energy (Fig. 2) [18]. Above T_S, Figs. 2(a1) and 2(a2) illustrate mainly a feature for the M_A band, and the M_B band is very weak, as depicted in Fig. 1. Once entering the SDW state, we clearly observed the splitting of the M_A band into the upper M_{A1} band, and the lower M_{A2} band, as shown by the dashed lines in Fig. 2(a3). With decreased temperature, this splitting increases quickly, and eventually reaches about 75 meV. Moreover, the M_B band also continuously goes deeper in binding energy. This dramatic temperature dependence and the sharp correlation with T_S prove that the electronic structure measured here reflects the bulk properties of the system with the same doping concentration. We note that one cannot identify whether the M_B band is gapped or not due to the strong M_{A1} band.

The temperature evolution of the bands around Γ is shown in Figs. 2(b1), 2(b2), 2(b3), 2(b4), and 2(b5). Below T_S, Γ_A band splits into Γ_{A1} (closer to Γ) and Γ_{A2} bands. The Γ_{A2} Fermi crossing is pushed away from Γ with decreasing temperature, while Γ_{A1} is slightly pushed downward in energy. The maximum splitting is about 35 meV in Fig. 2(b5). Meanwhile, band folding is observed as in the SDW state of Chromium [19]. The folded M_B band around Γ [Fig. 2(b5)] hybridizes with the Γ_B band near the Fermi level. The Γ_B band is slightly pushed down at low temperatures, and appears to be gapped from the Fermi energy by $\sim$25 meV. On the other hand, the folded M_B band around Γ [highlighted by an arrow in Fig. 2(b6)] seems still cross the Fermi energy, but the crossing is quite weak.

The downward movement of the M_B band suggest that it may be part of a pair of split bands. Indeed, the other split band is observed in data taken with randomly polarized light from a helium lamp, where a strong feature is present at M in the SDW state [Fig. 3(a)], while it is absent in Fig. 3(b) taken with elliptically polarized synchrotron light, illustrating strong polarization dependence of photoemission cross-section of the Fe 3d orbitals. In Figs. 3(c) and 3(d), the normal state data taken with the helium lamp exhibit the M_B band, while the M_A bands is strongly suppressed. In the SDW state [Figs. 3(e) and 3(f)], the M_B band clearly splits into two bands: one pushed to high binding energies as observed before in Fig. 2(a6), and the

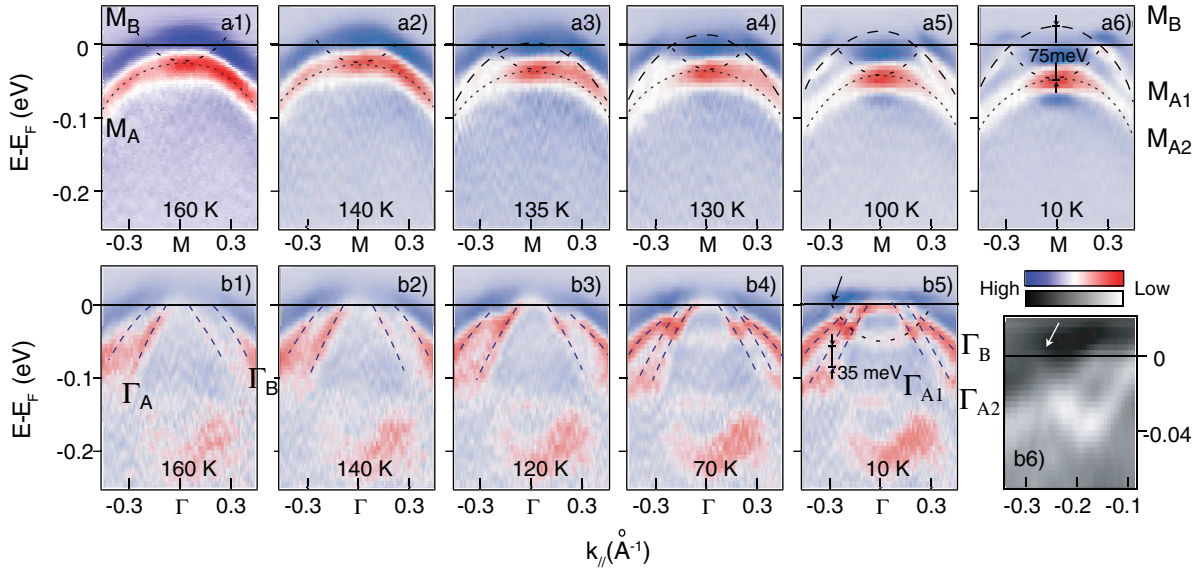

FIG. 2 (color). Temperature dependence of the electronic structure of $BaFe_2As_2$. Second derivative of photoemission intensity with respect to energy (a1)–(a6) along cut no. 2 in Fig. 1(a) at 160, 140, 135, 130, 100, and 10 K, respectively, and (b1)–(b5) along cut no. 1 in Fig. 1(a) at 160, 140, 120, 70, and 10 K, respectively. (b6) is an enlarged view of data in panel b5 near the Fermi crossing. Data were taken at the synchrotron with 21.2 eV photons. Dashed lines are the guides of eye for the bands, and band crossing effects are neglected for simplicity. Note the minimum of the second derivative represents the band.

other pushed to almost just at E_F (named hereafter as M_{B2} and M_{B1} band, respectively). The M_{B1} band crosses E_F, while the M_{B2} band does not show a crossing behavior. We observed the folding of the M_{B1} band to Γ as well (not shown). Furthermore, many photon energies have been exploited to explore the dispersion perpendicular to the FeAs plane and possible matrix element effects. We had not observed much dispersion along k_z direction [20]. As a result of these studies, the FS's in the SDW state are summarized in Figs. 3(a) and 3(b), which are much more complicated than the normal state ones. Around M, there are three FS's: the inner pocket corresponds to M_{B1}, and the FS's of M_{B2} (possibly gapped) and M_{A1} are almost coincident and barely resolved. Around Γ, there are four FS's corresponding to the two split Γ_A bands, and the folded M_{B1} and M_{B2} pockets. We note there are probably even more folded FS's that just could not be resolved in current experimental geometry.

The band structure calculation of the collinear SDW state of $BaFe_2As_2$ failed to reproduce the observed band splitting, and overestimated the magnetic moment to be about $2.3\mu_B$/Fe [16]. The 0.35% structural distortion of the lattice constants cannot account for the splitting energy scale either, plus there are no degenerate bands around M or Γ in the nonmagnetic ground state to split with. On the other hand, the splitting energy scales are comparable with the effective exchange interactions between the nearest and next-nearest neighbor effective local moments, which have been estimated to be 30–35 meV by comparing energies of

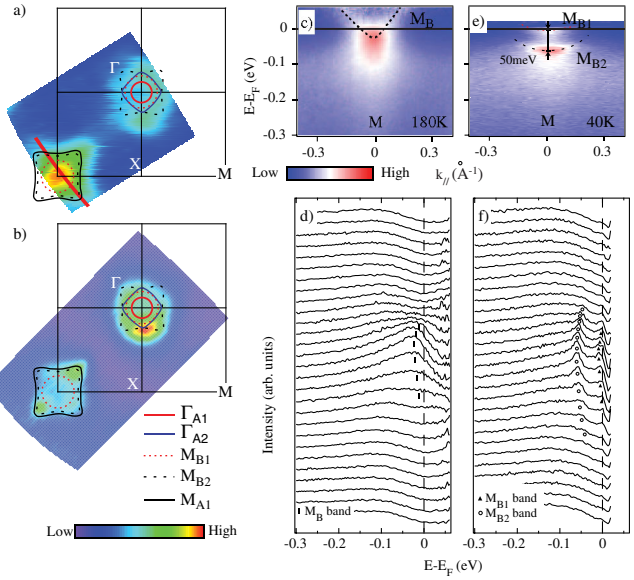

FIG. 3 (color online). Identification of the splitting of the M_B band. Photoemission intensity map taken (a) at 40 K with randomly polarized 21.2 eV photons, and (b) at 10 K with elliptically polarized 21.2 eV photons. The solid and dashed lines are guides of the eye for the measured hole-type FS's and electron-type FS's, respectively, in the SDW state. (c) Photoemission intensity at 180 K along the cut in panel (a), and (d) the corresponding EDC's. (e) and (f) present data taken at the same condition but at 40 K. Data in panels (c)–(f) have been divided by the resolution convoluted Fermi-Dirac distribution function to highlight the dispersions above E_F.

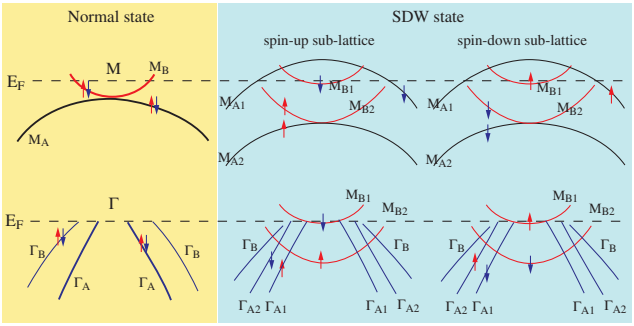

FIG. 4 (color online). Cartoon of the exchange splitting of the bands in $BaFe_2As_2$.

different spin configurations for $BaFe_2As_2$ [16]. This highlights the importance of local spin correlations, and the observed definite correlation between the splitting and T_S suggests exchange splitting might be the cause. The exchange splitting phenomenon has been widely observed in ferromagnets before [21]. To consider the exchange splitting in an SDW state, one could split the states into one configuration where spins are in phase with the SDW order, and the other out of phase with the order. For simplicity and illustration purpose, Fig. 4 views the SDW as two "ferromagnetic sublattices." Taking the spin-up sublattice, for example, the bands for majority (up spin) and minority (down spin) electrons are split in energy due to exchange interactions, which could naturally explain the complex band structure in the SDW state. Furthermore, it suggests that one could study the problem from the perspective of effective local moments [22–25], where the collinear SDW order is caused by the exchange interactions between the nearest neighbors and the next-nearest neighbors. Consequently, the SDW is naturally commensurate and does not require opening of a gap on the FS, or nesting of the FS's. This view may receive further support from the recent neutron scattering study that gives the ordered magnetic moment to be about $0.87\mu_B$ per Fe ion, which is difficult to be understood in a pure itinerant spin picture due to small FS's. One could then estimate one essential parameter of magnets, the Stoner ratio (i.e., the exchange splitting over magnetic moment). It is about 0.1 eV/μ_B for the M_A band of $BaFe_2As_2$, which is anomalously small, being only about 25% of that of Chromium and 10% of that of regular ferromagnets like bcc Fe [21].

Since the majority band is occupied by more electrons than the minority band, the total electronic energy is effectively saved when they are pushed equally in opposite directions. This suggests that the SDW and splitting could spontaneously occur. On the other hand, because the FS's around M and Γ are roughly apart by the SDW ordering wavevector (π, π), the nesting between them was suggested to lead to the SDW formation in pnictides [17,26], as in Chromium and its alloys [27]. Since possible signs of gap opening are observed on the Γ_B and M_{B2} FS's, the "Fermi-surface-nesting" mechanism might also play some role in the SDW formation. Although much more energy is saved through the exchange splitting than the gap opening, whether the exchange splitting is the primary cause of SDW, or driven by the FS nesting demands further exploration.

To summarize, we have observed large exchange splittings and possible gaps that stabilize the SDW state. Our results would shed light on the understanding of the relationship between the SDW and superconductivity, and set the foundation for further studies.

We thank Professors X. F. Jin and J. P. Hu for helpful discussions. This work was supported by the NSFC, MOST (National Basic Research Program No. 2006CB921300 and 2006CB922005), MOE, and STCSM of China.

*dlfeng@fudan.edu.cn

[1] Y. Kamihara *et al.*, J. Am. Chem. Soc. **130**, 3296 (2008).
[2] X. H. Chen *et al.*, Nature (London) **453**, 761 (2008).
[3] G. F. Chen *et al.*, Phys. Rev. Lett. **100**, 247002 (2008).
[4] Z.-A. Ren *et al.*, Mater. Res. Innovations **12**, 105 (2008).
[5] Z.-A. Ren *et al.*, Chin. Phys. Lett. **25**, 2215 (2008).
[6] M. Rotter, M. Tegel, and D. Johrendt, Phys. Rev. Lett. **101**, 107006 (2008).
[7] G. Wu *et al.*, Europhys. Lett. **84**, 27010 (2008).
[8] C. de la Cruz *et al.*, Nature (London) **453**, 899 (2008).
[9] X. F. Wang *et al.*, arXiv:0806.2452.
[10] Q. Huang *et al.*, arXiv:0806.2776.
[11] D. J. Singh and M. H. Du, Phys. Rev. Lett. **100**, 237003 (2008).
[12] G. Xu, W. Ming, Y. Yao, X. Dai, and Z. Fang, Europhys. Lett. **82**, 67002 (2008).
[13] I. I. Mazin, D. J. Singh, M. D. Johannes, and M. H. Du, Phys. Rev. Lett. **101**, 057003 (2008).
[14] C. Cao, P. J. Hirschfeld, and H.-P. Cheng, Phys. Rev. B **77**, 220506(R) (2008).
[15] F. Ma and Z. Y. Lu, Phys. Rev. B **78**, 033111 (2008).
[16] F. Ma, Z. Y. Lu, and T. Xiang, arXiv:0806.3526.
[17] J. Dong *et al.*, Europhys. Lett. **83**, 27 006 (2008).
[18] Th. Straub *et al.*, Phys. Rev. Lett. **82**, 4504 (1999).
[19] E. Rotenberg *et al.*, New J. Phys. **7**, 114 (2005).
[20] At certain photon energies, some more subtle features were observed. Since it is independent of the arguments made here, we leave it for future further investigations.
[21] F. J. Himpsel, Phys. Rev. Lett. **67**, 2363 (1991).
[22] F. Ma, Z. Y. Lu, and T. Xiang, arXiv:0804.3370.
[23] T. Yildirim, Phys. Rev. Lett. **101**, 057010 (2008).
[24] C. Fang, H. Yao, W.-F. Tsai, J. P. Hu, and S. A. Kivelson, Phys. Rev. B **77**, 224509 (2008).
[25] S. P. Kou, T. Li, and Z. Y. Weng, arXiv:0811.4111.
[26] M. M. Korshunov and I. Eremin, Phys. Rev. B **78**, 140509 (R) (2008).
[27] E. Fawcett, Rev. Mod. Phys. **60**, 209 (1988).